

## SEPARATOR TECHNOLOGY IN LI-ION BATTERIES: MATERIALS, FABRICATION TECHNIQUES, AND PERFORMANCE TESTS

**Nikolas Krisma Hadi Fernandez**

Department of Mechanical Engineering, Faculty of Engineering and Technology, Sampoerna University  
Department of Mechanical Engineering, Faculty of Mechanical Engineering and Manufacturing  
Universiti Tun Hussein Onn Malaysia  
Email: nikolas.fernandez@my.sampoernauniversity.ac.id

**Farid Triawan**

Department of Mechanical Engineering, Faculty of Engineering and Technology, Sampoerna University  
Email: farid.triawan@sampoernauniversity.ac.id

### ABSTRAK

Tren penggunaan kendaraan listrik semakin hari semakin meningkat. Dengan meningkatnya penggunaan kendaraan listrik, maka diperlukan penguasaan teknologi kunci yang digunakan oleh kendaraan listrik tersebut, salah satunya adalah baterai, khususnya baterai ion litium (BIL). Terdapat banyak komponen penting yang ada di BIL, salah satunya adalah bagian separator yang berfungsi untuk menghalangi terjadinya arus pendek (korsleting) antara anoda dan katoda baterai sambil memberikan jalan agar pertukaran ion dapat berlanjut. Artikel ini bertujuan untuk merangkum informasi-informasi penting yang berhubungan dengan teknologi separator pada baterai ion litium. Pembahasan dimulai dengan material apa saja yang telah digunakan dalam membuat separator pada produk baterai komersial dan baterai yang masih dalam tahap penelitian dan pengembangan. Selain itu, teknik fabrikasi separator dengan cara konvensional dan cetak 3-Dimensi juga didiskusikan. Terakhir, artikel ini memaparkan beberapa studi lampau tentang cara-cara melakukan uji performa terhadap material separator.

**Kata kunci:** separator baterai, fabrikasi, material, uji performa, baterai ion litium.

### ABSTRACT

*The trend of using electric vehicles is increasing. With the increasing use of electric vehicles, it is necessary to master the key technologies used by electric vehicles, one of which is batteries, especially lithium-ion batteries (LiB). There are many important components in the LiB, one of which is a separator that serves to block short circuits between the anode and cathode of the battery while providing a way for ion exchange to continue. This article summarizes important information related to battery separator technology. The information includes the materials that have been used in commercial products and those of under research and development. In addition, the method of fabricating the separator using conventional methods and 3D printing is discussed. Finally, this article also discusses how several studies perform performance tests on separator materials.*

**Keywords:** battery separator, fabrication, materials, performance test, lithium-ion battery.

### 1. INTRODUCTION

The trend for electric vehicles continues to grow. Sales of electric vehicles in 2021, for example, will double to 6.6 million units compared to 2020 [1]. This sales record makes electric cars hold a market share of almost 10% of all car sales in 2021, four times more than in 2019. It has been predicted that fossil fuel vehicles will be replaced by electric vehicles in 2025 [2]. According to Subekti et al., five key technologies must be considered in developing electric vehicles: driving experience and maintenance, batteries, electric motors,

electronic control systems, and battery charging systems [3]. The battery is one of the most critical parts of an electric vehicle. This is because the cost of making the battery contributes around 25–40% of the cost of making electric vehicles [4], [5].

There are several types of battery materials used in electric vehicles. These types of batteries include lead-acid, nickel-metal hybrid, and lithium-ion [6], [7]. Each of these battery types has its advantages and disadvantages. However, from these three types of batteries, the lithium-ion battery type (from now on referred to as LiB) is the type that has the best properties for use in electric vehicles [2], [8]. This is because LiB has a high efficiency, long life cycle, and high-power density [7], [9], [10].

Figure 1 shows the components in the LiB, namely, the cathode, anode, separator, and electrolyte [11]. The anode and cathode are opposing the electrodes, where electrons will flow from the anode to the cathode, and lithium ions will flow from the cathode to the anode when the battery is used. The opposite occurs when recharging occurs. The electrolyte is a material that acts as a bridge for lithium ions to move between the anode and cathode. Finally, the separator is the part that keeps the anode and cathode from touching and causing a short circuit [12]–[14], however it still provides space for lithium ions to move between the electrodes. This article will focus on the separator part.

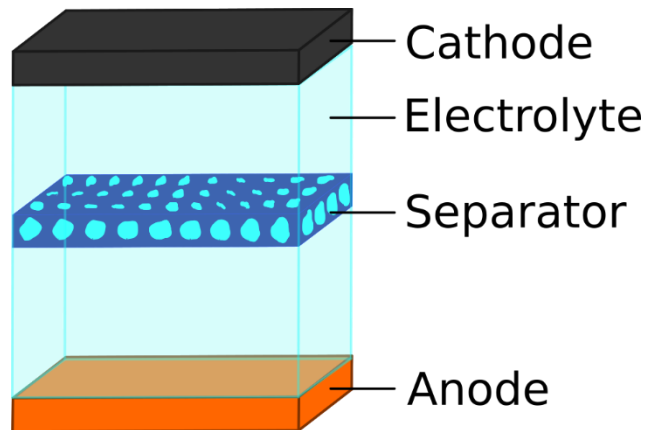


**Figure 1. Battery components**

The purpose of this article is to provide the latest and important information regarding separator battery technology. This includes several materials that have been, or are being, developed for commercial separators and the fabrication techniques using conventional and 3-dimensional (3D) printing techniques. In addition, information on how to conduct the performance test for evaluating a separator material is also provided. This knowledge can be helpful for researchers who are developing new separator materials by 3D printing method, and learning how to evaluate the samples' performance.

## **2. BATTERY SEPARATOR CHARACTERISTICS AND MATERIALS**

### **2.1 Characteristics and Properties of Battery Separator**

The general specifications of a battery separator can be seen in Table 1. These specifications are divided into several types, which are chemical, physical, and mechanical characteristics with a minimum value that a battery separator must possess. These specifications include minimum mechanical strength, pore percentage, size, and so on [15], [16].

**Table 1. Minimum specification of a lithium-ion battery separator [16]**

Parameter	Score
Chemical and electrochemical stability	Stable for a long time.
wettability	Gets wet quickly and thoroughly.
Mechanical strength	> 98.06 MPa.
Thickness	20 – 25 $\mu\text{m}$ .
Pore size	< 1 $\mu\text{m}$ .
Pore percentage	40 – 60% of the total volume.
Permeability	< 0.025 $\text{s} \cdot \mu\text{m}^{-1}$ .
Temperature stability	Shrinkage < 5% when placed in a 90°C environment within 60 minutes.
shutdown function	Can turn off the battery when the temperature is critical automatically.

The first characteristic that is important for battery separators is the stability of their chemical structure. The separator must have a stable chemical structure, which means it will not react to the battery's reactions. In addition, the separator must also be able to absorb the electrolyte used in the battery. As a result, the separator will have low resistance and high conductivity.

The second important property of the battery is the wettability of the separator. This wettability property is related to the nature of the separator, which can absorb liquid electrolytes to facilitate the ion exchange process in the battery. The better the separator absorbs the liquid electrolyte, the smaller the resistance value and the greater the ionic conductivity of the separator [16]–[18]. Measuring wettability is usually done in two ways, namely by looking at the electrolyte's contact angle and absorption capacity.

The contact angle can show the liquid's ability to be absorbed into a material. In the separator experiment, the liquid used is a liquid electrolyte. This liquid electrolyte will be dripped into the separator, and its distribution will be observed [19]. Generally, a suitable separator has hydrophilic properties (Figure 2). How to measure the contact angle will be explained in the fourth chapter.

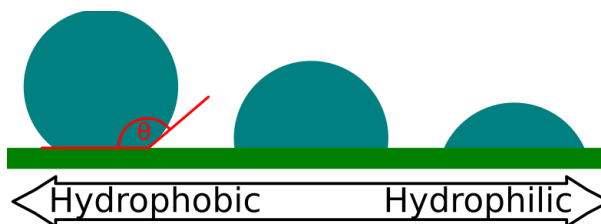


**Figure 2. Illustration of the contact angle of the electrolyte on the separator with hydrophobic to hydrophilic properties**

In addition to the contact angle, the wettability of the separator can also be measured by finding the value of the electrolyte absorption capacity. This value can be found by measuring the mass of the separator before and after immersing it in a liquid electrolyte for two hours [17]. Furthermore, the value of electrolyte absorption capacity (EAC) can be found using Equation (1) [20]–[22].

$$\text{EAC (\%)} = \frac{W_1 - W_0}{W_0} \times 100\% \quad (1)$$

where,  $W_0$  and  $W_1$  is the mass of the separator before and after being immersed in the liquid electrolyte. The higher the EAC value, the better the ability of the separator to absorb electrolytes [17]. That is, the better the performance as a separator.

The third property of the separator that needs attention is its mechanical properties. The minimum tensile strength of the separator with a thickness of 25  $\mu\text{m}$  is 98.06 MPa. This value usually occurs during the battery assembly [16], [23]. In addition, the separator must also withstand punctures due dendrite that may formed during battery usage. Next, thickness of commercial separator is 20 – 25  $\mu\text{m}$  for commercial and 10  $\mu\text{m}$  or less for new applications, such as electric vehicles. The thinner the separator, the smaller the value of the resistance. In addition, the thinner the separator, the more space can be used by the battery so that the battery capacity increases [16].

The fourth important specification is the pores of the separator. The pores aim to facilitate the exchange of ions between the electrodes. The pore must be large enough for ions to flow but not so large that a short circuit can occur. Furthermore, the recommended pore percentage to separator volume is around 40 – 60%. The calculation of the pore percentage can be done in two ways, namely by using the ratio between the volume of the space and the geometric volume (Equation (2)), and the ratio between the weight of the separator before and after absorbing liquid (Equation (3)) [16].

$$\text{Pore (\%)} = \left(1 - \frac{\rho_V}{\rho_P}\right) \times 100\% \quad (2)$$

$$\text{Pore (\%)} = \left(\frac{W_1 - W_0}{\rho_L V_0}\right) \times 100\% \quad (3)$$

where  $\rho_V$ ,  $\rho_P$ , and  $\rho_L$  are the densities of the separator, polymer material, and liquid used. Next  $V_0$  is the volume of the separator before the liquid is immersed. Lastly,  $W_0$  and  $W_1$  is the mass of the separator before and after being immersed in the liquid. In practice, the second way is more often used than the first way.

In addition to the pore percentage, an even pore layout is also recommended. Uneven pore layout can cause uneven current density. This can lead to dendrites forming, damaging the separator and the battery as a whole [24] – [27].

The fifth property to note is the permeability of the battery separator. This property is the ratio of the resistance of the separator after being immersed in the electrolyte and the resistance of the electrolyte itself. In general, this value is usually less than  $0.025 \text{ s} \cdot \mu\text{m}^{-1}$  as measured by ASTM D726 and D737 [16].

The sixth important property is the temperature property of the separator. The stability of the separator temperature can be seen from the shrinkage rate of the separator. The way to find the shrinkage level of the separator is to measure the size of the separator before and after it is placed in a room with a certain temperature and a certain time. The standard shrinkage of the separator is 5% of its initial size after being placed in an environment with a temperature of  $90^\circ\text{C}$  for 60 minutes. Higher shrinkage can put a voltage on the separator, which can eventually cause a short circuit. Calculation of the percentage of shrinkage can be done using Equation (4) [17], [20].

$$\text{Shrinkage (\%)} = \left(\frac{A_0 - A_1}{A_0}\right) \times 100\% \quad (4)$$

where,  $A_0$  and  $A_1$  are the separator areas before and after being heat treated for some time.

The last important characteristic or function is the shutdown function. This function exists when the separator is at a high temperature. At this temperature, the separator will melt and close its pores, so the ion exchange process will stop. This must be considered when choosing a new material to research or modifying the separator's design.

## 2.2 Battery Separator Materials

When viewed from the perspective of the use of separator membrane materials, the design phase of the separator can be divided into three phases [13]. The first phase is polyolefin-based separators, for example, polyethylene (PE) and polypropylene (PP). This first-phase separator has many pores and is an insulator [14]

but is susceptible to development of dendrites from the lithium component due to using a liquid electrolyte [28]. Furthermore, the second phase separator is a separator whose surface has been given an additional layer. This layer gives the separator better temperature stability and strength [29]. However, this separator still uses a liquid electrolyte, so the risk of dendrite development still exists [13]. Therefore, solid electrolytes and separators can reduce the risk of dendrite development [30].

For commercial separators, the material used is usually a polyolefin-based [31], [32], namely polyethylene (PE) and polypropylene (PP). Therefore, it can be said that commercial separators are still in the first phase. Some separators get a special coating on their surface that makes them eligible for the second phase. Some of the materials used by commercial separators can be seen in Table 2.

**Table 2. Commercial separator materials**

Company	Material	Ref.
Celgard	PP, PE, and three layers of PP/PE/PP	[33]
ENTEK Membranes LLC	<i>Ultrahigh molecular weight polyethylene</i> (UMWPE)	[34], [35]
Asahi Kasei	PE, PP	[36]

Apart from commercial separators, there are several other materials that many researchers investigate. Xiaoyu Jiang et al., for example, attempted to create a separator using Polylactic Acid (PLA) as the main material and a shell of Poly-Butylene Succinate (PBS) [37]. PLA was chosen because of its mechanical strength, temperature stability properties, and dimensions. Meanwhile, PBS was chosen because of its affinity with liquid electrolytes and lower melting temperature than PLA. This melting temperature is intended for the shutdown function, where PBS will melt and close the pores while PLA will maintain product integrity. In addition, separators with this material can provide less resistance compared to separators coated with ceramic.

JC Barbosa et al. investigated a separator containing the primary ingredient PLA, specifically Poly L-Lactic Acid (PLLA) [22]. This PLLA was dissolved in a mixture of dichloromethane (DMC) and dimethylformamide (DMF) with a volume ratio of 70:30 at room temperature.

Chengyai Cai et al. investigated a separator made primarily of PLA and then coated with various materials [21]. The materials used as coatings are polydopamine (PDA) and zeolitic imidazolate frameworks (ZIF). The results of the journal research show that PLA with PDA and ZIF coatings increases the stability of battery cycles and restrains dendrite growth. Furthermore, the electrolyte absorption rate is higher when compared to PLA, which is only coated with PDA or PLA, which is not coated at all.

Satita Thiangtham et al. studied separators, with the main ingredient being biomembranes mixed with sulfonated cellulose (SC) [17]. This biomembrane was created by dissolving PLA/PBS biocomposite into DMF. Mixing the biomembrane and SC results in a pore percentage level of up to 87.7% with a pore diameter of about  $1.4 \pm 0.6 \mu\text{m}$ . Finally, compared to the commercial product Celgard 2400, this material can provide a higher discharging capacity and better cycle performance with a more stable battery capacity.

Yang Liu et al. studied battery separators with boron-nitride (BN) materials [38]. This separator has stable battery cycle performance and high Coulombic efficiency. In addition, this separator also has stable electrochemical properties and maintains a high specific capacity compared to commercial separators.

Liao et al. investigated a flame retardant separator with suitable ionic conductivity [39]. This separator was created with bacterial cellulose (BC) combined with attapulgite (ATP), so it has a high EAC of 470.03% and an ionic conductivity of 1.734.

Qian et al. are researching stretchable batteries. All battery components, from the anode, and cathode, to the separator, are 3D printed with the primary material, nano-fibrillated cellulose (NFC) [40]. The battery can be stretched 50% back and forth with the addition of only 3% electrode resistance after 50 stretches. Other studies usually use polyolefin materials with new layers or mixtures with other materials.

### 3. BATTERY SEPARATOR FABRICATION PROCESS

The battery separator fabrication process can be divided into conventional and new processes, such as 3D printing method. The conventional process is normally used to manufacture battery separators for commercial purposes. Another fabrication method is currently being researched and attracted many attention is to create a battery separator by 3D printing machine.

### 3.1 Conventional Fabrication Method

There are two methods for producing conventional battery separators: dry and wet. The fundamental difference between these two methods occurs during the primary material melting process. The melting process of the dry process is done without using any mixture. Meanwhile, a mixture of hydrocarbons is used during melting process at the wet process.

The dry process for the separator fabrication begins by melting the polyolefin material as the primary material [41]. The main material usually used in this process is PP. Next, the melted polyolefin is cast into a film layer, while annealing is carried out at a temperature between the glass transition temperature and the melting temperature. This is done so that the crystallization of the separator can be controlled. During this process, the separator will be pulled in the direction of the machine (machine direction, MD). Because the direction of pull is only on one axis, the pore shape of this process is usually like a torn cloth (as in Figure 3a) [14], [42], [43]. In addition, the tensile strength of the separator concerning the MD and the transverse direction (TD) is also different.

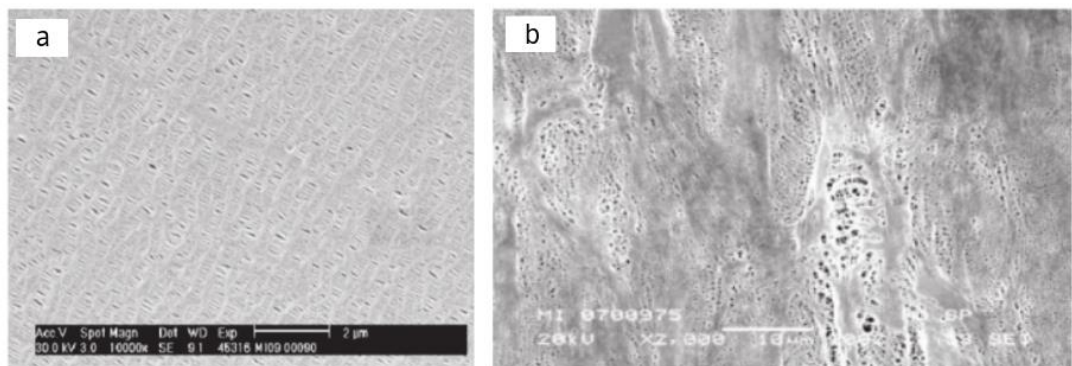


**Figure 3. SEM image of the separator fabricated using (a) dry and (b) wet processes. Reprinted from reference [42], with permission from AIP Publishing (copyright belongs to AIP Publishing)**

One of the solutions for the geometric shapes and differences in the tensile strength of the separators can be solved by pulling the separators in both directions during the fabrication process. Several researchers have studied and used it [43-46]. However, the drawback of this two-way pull technique is the size and distribution of the pores formed. The size that forms is usually relatively large, with a non-uniform distribution [44]. Another way is to pull the separator into a controlled MD and TD. That is, when the separator is pulled to TD, at the same time, the pull to MD is controlled so that relaxation occurs [47]. This results in a separator with a pore shape close to a circle and an aspect ratio close to 1 [41].

In addition to the dry process technique, another popular technique is the wet process with a two-way separator pull [42]. In this process, polyolefin (usually PE) is mixed with a liquid additive, for example, a hydrocarbon, at a temperature above its melting temperature. Next, this mixture is cast into a film layer and drawn onto the MD and TD. Next, the liquid hydrocarbon is evaporated with the evaporating solution to produce pores in the separator (see Figure 3b). The most commonly used hydrocarbon liquid is methylene chloride, while the most commonly used vaporizing solution is paraffin oil [19]. This evaporation process usually increases the cost of separator fabrication with a wet process. The advantages of this process over MD

and TD are the more uniform pore structure and tensile strength. In addition, the tensile strength of the separator from this process is relatively higher [41].

### 3.2 Fabrication 3D Printing Techniques

Several techniques can be used to fabricate battery separators using 3D printing techniques. Zhiyang Lyu, et al. provide four techniques that can be used to print battery components, including the separator. These techniques or technologies are Direct Inject Writing (DIW), Fused Deposition Modeling (FDM), Inkjet Printing (IJP), and Stereolithography (SLA) [48]. The four technologies can be seen in Figure 4.

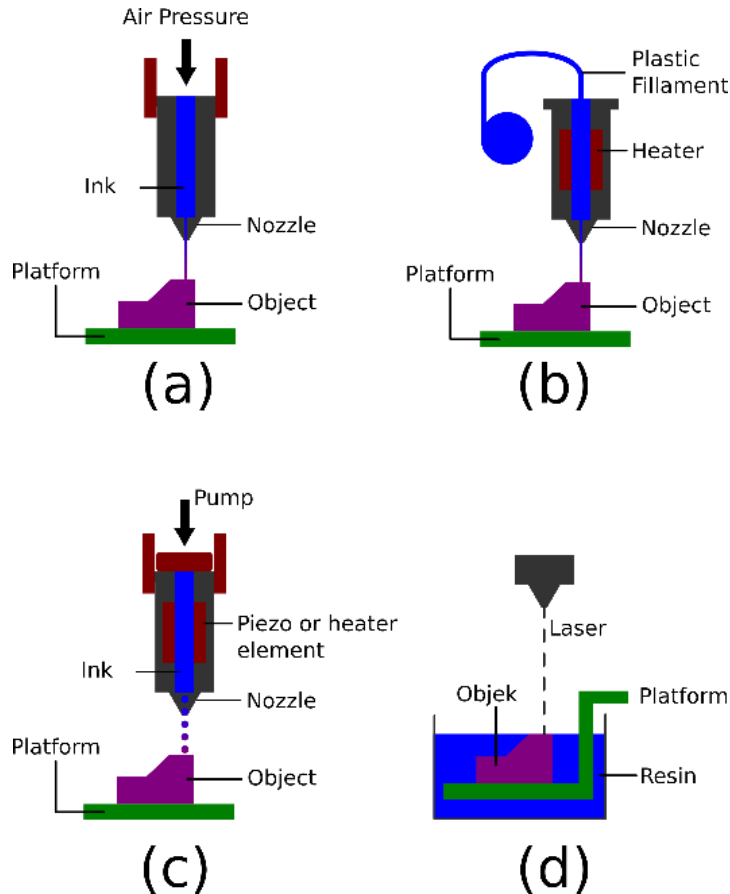


**Figure 4. 3D printing technology: (a) DIW, (b) FDM, (c) IJP, and (d) SLA**

Several studies are using the DIW technique to print the battery separator. Ji Qian et al. printed stretchable batteries [40]. In addition, Yang Liu et al. printed a separator with BN material [38]. Both of these studies used the same tool to print their separators, namely the Fisnar F4200N robot, with the thickness of the separator controlled by the Fisnar DSP501N, a wind-powered liquid dispenser.

Apart from fabrication using the DIW technique, several studies use the FDM (fused deposition modeling) technique to make their separators. This technique is more limited because it requires a thermoplastic material as a filament to print objects. Maurel et al., for example, succeeded in printing a separator with several shapes and filling density experiments in the mold [49]. This study uses FDM technology using the Prusa i3 MK3 engine. Meanwhile, the filament is self-formulated, using PLA as the

primary material. In addition, Reyes et al. also use the FDM technique to print their batteries [50]. In this research, the researchers printed the battery in one mold, starting from the cathode current collector, cathode, separator, anode, and anode current collector.

#### 4. BATTERY TEST SEPARATOR PERFORMANCE

Research and development of separator materials for batteries requires performance testing techniques for the separator itself, especially if the separator is made of a new material. Performance testing of the separator can be seen from the mechanical performance (tensile and compressive strengths), geometric performance (number of pores, thickness, wettability, and temperature stability), and electrochemical performance (internal resistance, ionic conductivity, and cycle performance). In addition, in the separator research, morphology and chemical bonding tests of the separator were also carried out. This is usually done using a scanning electron microscope (SEM) and a device that supports Fourier transform infrared (FTIR). Before that, it is necessary to know the failure modes that can occur in the separator, especially mechanical failure modes.

##### 4.1 Failure Characteristics

The failure mode of a battery is when a short circuit occurs. A short circuit on a battery can occur when the separator can no longer carry out its duties to separate the anode and cathode of the battery. The separator is said to have failed if the battery has a short circuit. This separator failure can occur when the separator fails mechanically, has enlarged pores, or has tear in the separator body. This may occur due to dendrites growing on the separator [24], [25] or because an external load is too high.

Chunhao Yuan et al. proposed a universal failure mode in battery separators [51]. This failure mode is defined using the strain of the separator tested by compression test. The primary strain data  $e_j$  ( $j = 1, 2, 3$ ) received will be converted to strain data in the logarithmic range. The conversion of the principal strain values of the technique into strains in the logarithmic range can be seen in Equation (5).

$$\varepsilon = \ln(1 + e) \quad (5)$$

After getting the strain value within the logarithmic range, the next step is to see if the battery separator will fail. This is done by calculating the volumetric strain ( $\varepsilon_V$ ) and equivalent strain ( $\varepsilon_{eq}$ ). These two variables are calculated using Equations (6) and (7).

$$\varepsilon_V = \varepsilon_1 + \varepsilon_2 + \varepsilon_3 \quad (6)$$

$$\varepsilon_{eq} = \sqrt{\frac{1}{2}[(\varepsilon_1 - \varepsilon_2)^2 + (\varepsilon_2 - \varepsilon_3)^2 + (\varepsilon_3 - \varepsilon_1)^2]} \quad (7)$$

where  $\varepsilon_j$  ( $j = 1, 2, 3$ ) is the  $j$ -th principal strain. Furthermore, these two variables can be compared with the failure limit value of a battery. Chunhao Yuan et al. recommended the failure limit values as shown in Equations (8) and (9) [51].

$$\varepsilon_V = -2.11 \quad (8)$$

$$\varepsilon_{eq} = 2.13 \quad (9)$$

Both the volumetric strain ( $\varepsilon_V$ ) and equivalent strain ( $\varepsilon_{eq}$ ) can be used as a reference when analyzing the mechanical strength of the battery separator materials. This analysis can be carried out when experimenting with new materials for battery separators by looking at the strength of the separator itself. The maximum load and safety factor that can be applied to the separator can be calculated with the reference strain obtained.



The battery separator may fail over time. This means battery separators must be tested before it is approved for commercial use. This is to ensure that the product is safety and suitable for the designated battery's lifetime. As one of the critical components in battery structure, the separator's performance certainly affects the performance of the battery itself. For example, a concentrated pore can lead to a concentrated current density. This can lead to the growth of dendrites, which can damage the separator and eventually creates a short circuit [24]–[27]. Therefore, a separator must follow the standard performance to provide good endurance.

Due to the reasons above, performing the performance tests on a separator is a must. Next, it will be explained the apparatus and experimental tools used in the performance tests, the variables measured, and the practical procedures that are carried out.

## 4.2 Performance Test Experiments

The separator performance test can be divided into two parts. First is the mechanical performance test, which is about the strength of the material used by the separator. The second is a functional performance test, which is about the performance that the separator can provide. Number of pores, separator barriers, ion exchange functions, and so on are examples of these functions.

### 4.2.1 Testing Apparatus

The testing apparatus used depends on the test to be carried out. Starting with testing geometry, morphology, and chemical structure, from geometry, morphology, and chemical structure (electrochemistry) to mechanical testing of the separator. Please note that the apparatus mentioned in this section is the apparatus in general. More specific apparatus, such as brand and type, will be mentioned in the next sub-chapter. Figure 5 shows some of the typical apparatus used to test the performance of the battery separator, namely for mechanical testing, electrochemical testing, and the geometry and morphology of the separator. These images were obtained from these resources: [52]–[54].

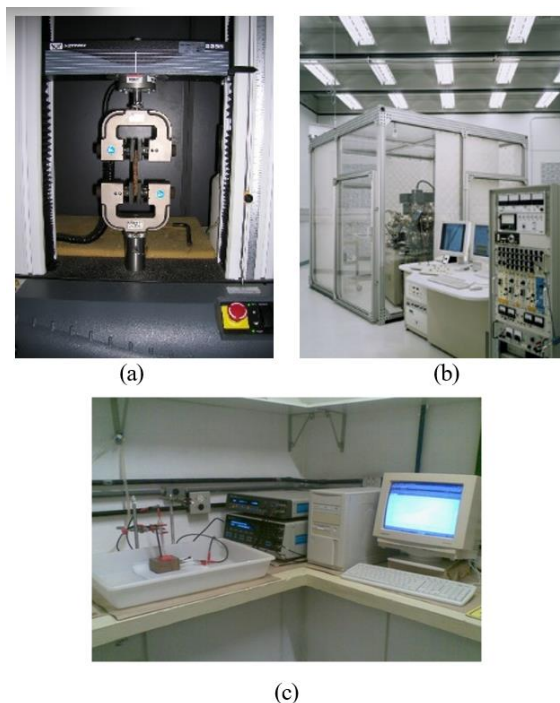


**Figure 5. Some separator testing apparatus: (a) tensile test machine (Kerina Yin [53]), (b) scanning electron microscope [52]), and (c) electrochemical impedance spectroscopy [54])**

First, the apparatus for mechanical testing. Mechanical testing is typically used to determine the strength of the object being tested, in this case, the separator. Accordingly, this testing apparatus is a tensile and compression testing machine.

Second, the apparatus for electrochemical testing. Apparatus included in the electrochemical testing process are electrical testing instruments and batteries. They start from resistance testers and electrochemical impedance spectroscopy meters to battery charging and discharging testing systems. In addition, coin or button battery assembly kits are required for this test.

The last is the geometric and morphological performance of the separator. In testing this performance, some of the apparatus needed are a length measurement instrument, mass measurement, contact angle testing, a scanning electron microscope (SEM), and a device that supports Fourier Transform Infrared (FTIR). To perform length and mass measurements, standard devices can be used. Specifically for length measurements, the instruments used can be a ruler (to measure the area of the separator) and a micrometer (to measure the thickness of the separator). Other apparatus that can assist with testing may also be used. For example, time counters, temperature gauges, sample storage containers, and cutting tools.

#### 4.2.2 Variables that Need to be Measured

Several variables need to be measured to determine the performance of the separator being studied. These variables can be divided into three categories, namely mechanical, electrical, and geometric performance.

Mechanical performance can be seen from the strength of the material used to make the battery separator. The mechanical strength of the separator can be seen from the maximum load that can be applied before the equivalent strain and the resulting volumetric strain are more than the failure limit value [51]. The variables that need to be measured for mechanical performance are the stress and strain values of the separator being tested. These two variables can be measured using a universal test machine. Example of these machines are the Instron 1121 [20] and the DMA Q800 Dynamic Mechanical Analyzer [55].

A separator's electrical and chemical performance can be seen from its internal resistance, ionic conductivity, and cycle performance. All tests can be carried out with a testing system for each variable using different apparatus. The universal electrochemical testing apparatus can perform the internal resistance test. For example, the Ivium-n-Stat device from the Ivium company in the Netherlands can be used for this application [20]. Ionic conductivity can be analyzed by measuring electrochemical impedance spectroscopy (EIS). EIS measurements can be performed with various devices, such as Gamry Reference 3000 [55], Gamry Reference 600+ [21], Autolab PGSTAT-12 (Eco Chemie) [22], and  $\mu$ Autolab Type III impedance spectrometer [17]. EIS measurements of the tested battery can produce large resistance values [56]–[58]. This value is then used to find the ionic conductivity value ( $\sigma$ ) using Equation (10).

$$\sigma = \frac{t}{R_b A} \quad (10)$$

where  $\sigma$  is the ionic conductivity ( $S/cm$ ),  $t$  is the thickness of the sample ( $cm$ ),  $R_b$  is the resistance ( $\Omega$ ), and  $A$  is the contact area of the electrode used ( $cm^2$ ) [17], [55].

Separator performance can also be measured by the cycle performance of the battery with the separator being tested. This performance is measured by measuring the charging and discharging capabilities of the battery. This performance test is carried out with a battery testing system with a C ratio of 0.05 – 2C ( $1C = 170mA/g$ ) with a voltage of around 2.5 – 4.2 V. Some of the battery testing system devices are the LAND battery test system [20], LANHE battery test system [21], Bilogic VMP [22], and Battery Charge/Discharge System HJ Series (Hakuto/Denko, Japan) [17].

The geometric performance of the separator can be seen from the several geometric shapes of the fabricated separator being tested. The geometry includes thickness, number of pores, wettability, and temperature stability. The separator's thickness is typically in the 20-25  $\mu m$  range. Therefore, we need a device capable of measuring such a thin thickness. Fortunately, micrometer measuring devices are sufficient for use according to the standard.

Several variables that need to be measured to examine the separator's geometric performance are the separator's mass and volume. These two variables can be used to find the separator's pore percentage and EAC performance. The trick is to measure the mass of the separator before and after it is immersed in the liquid electrolyte. Equation (1) can be used to calculate EAC performance. After that, the pore percentage can be found by knowing the volume of the separator before it is immersed and the density of the liquid electrolyte used. Then, the pore percentage can be found using equation (3).

For wettability, the variable that needs to be measured is the contact angle. Dripping liquid electrolytes can measure the contact angle on the separator. Furthermore, the contact angle can be measured, as shown in Figure 2, using a contact angle measuring instrument, such as the Kruss DSA 100E [59] or the Attension Theta series [60]. Several standards that can be used to measure this contact angle are ISO 19430, ISO 15989:2004, ASTM C813-90, and ASTM D7334-08 [61].

Another test usually carried out when testing the separator is the morphology of the material used. The first test was by SEM to analyze the pore surface and thickness [62]. Some of the SEM devices that can be used are JEOL JIB 4610F [63], SEM SU3500 [64], Hitachi S-4800 [17], FEI Quanta 600-series [22], [55], and FE-SEM XL-30 [20]. An example of the results of morphological testing can be seen in Figure 3.

The tester can also identify the polymer structure and chemical bonds of the separator being tested by FTIR testing. This test can be carried out with various devices that support infrared spectroscopy for FT with a wave measurement distance of about  $400 - 4000 \text{ cm}^{-1}$  [20]–[22]. An example of the results of testing the chemical bond structure can be seen in Figure 6 taken from [65].

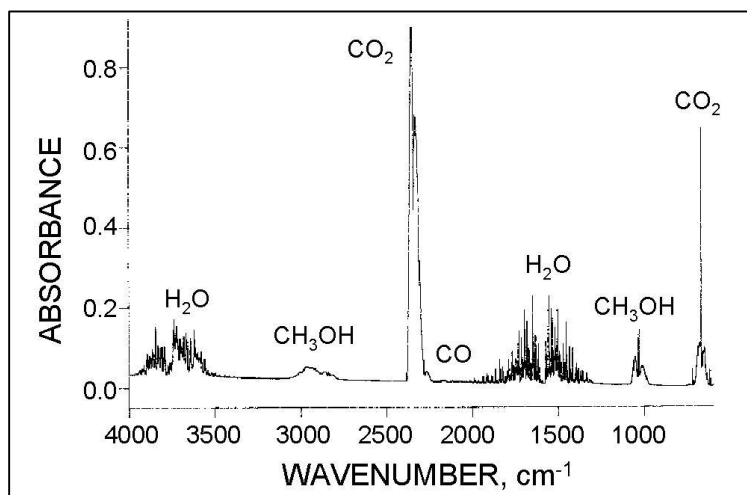
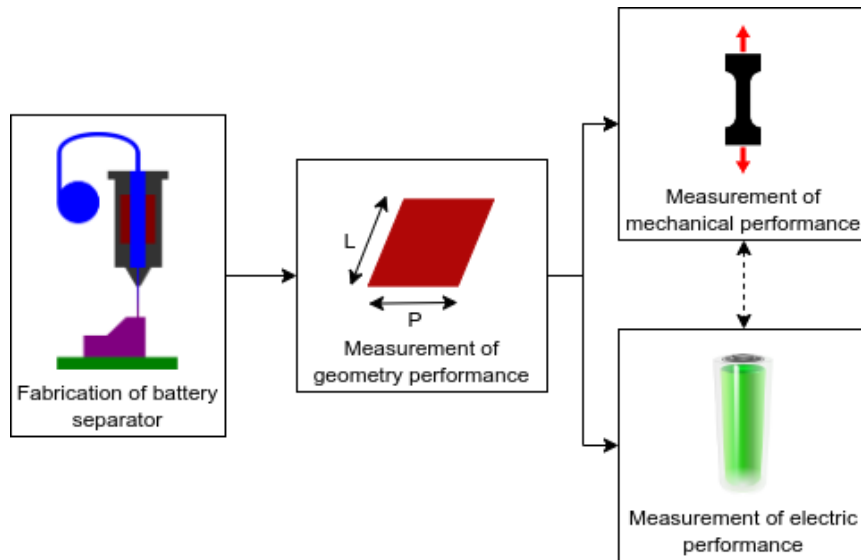


Figure 6. Example of an FTIR chart [65]

#### 4.2.3 Experimental Steps

Several steps must be taken to carry out experiments related to the LiB separator. These experimental steps can be done all at once, in part, or added according to the purpose of the experiment. In general, the practical steps can be seen in Figure 7. The first step is fabricating a battery separator using the selected technique, for example, 3D printing using the FDM technique. After fabrication is the measurement of the geometry of the separator, starting from the area, thickness, number of pores, and so on. After that, measurements of the mechanical and electrical performance of the separator can be carried out. These two measurements can be performed in parallel or only partially.



**Figure 7. Experimental steps for a battery separator**

First, separator fabrication. This includes selecting materials, new design trials, and new fabrication methods. This means that the formulation of the material, preparation before use, the fabrication plan, and the use of the material as a separator are included in the first step. For example, suppose the research is to use a PLA material with the addition of a new material as the main material in making a separator using a 3D printer. In that case, the first steps include formulating the material mixture, preparing the material as a filament, and 3D printing. Please note that the variables used in this process must be documented. These variables include machines used for material formulation, filament manufacturing (for fabrication by 3D printing), 3D printing, and variables while printing separators (bed temperature, print speed, slicer software, and so on). It is intended that the results of separator fabrication can be carried out again. In addition, some experimental processes require the destruction of the separator membrane. Therefore, more than one sample with the same variable is needed to ensure experimental validation. In addition, a morphological test of the separator can also be carried out to ascertain the chemical content of the material used.

Second, measurement of separator geometry performance. In this stage, all the geometric performance measurements that have been fabricated are carried out. This includes thickness, pore number, size, wettability, EAC performance, material composition, chemical structure, morphology, and temperature stability. Several geometric performances can be measured simultaneously using the same measurement data. For example, suppose the researcher knows the density of the liquid electrolyte. In that case, the number of pores and performance properties of EAC can be estimated using data on the mass of the separator before and after immersion in the same liquid electrolyte. Other performance measurements can refer to the measurements of each variable required in the previous sub-chapter.

Third, measurement of mechanical performance. As the name suggests, in this section, the performance regarding the mechanical strength of the separator is measured. It starts from the MD and TD's tensile strength to the separator's compressive strength. It aims to measure the maximum load given to the separator.

Fourth, electrical performance measurement. Please note that measuring the electrical performance of the separator requires battery assembly using anode, cathode, and other battery components that is necessary. In addition, because the device being tested is a separator, the material and fabrication process of the anode, cathode, and other components must be the same between the separator samples. This is so that there are no errors in the performance data of the separator itself. In some measurements, especially when measuring battery cycle performance, tests are carried out with button battery assemblies of type 2025 or 2032 [17], [20]. One of the reasons why performance measurements are made on button battery assemblies is to reduce other variables that might affect the measurement, such as dendrites [66],[67].

#### 4.2.4 Performance Test Results from Several Sources

As a reference, table 3 summarizes the performance tests that done by several researches. Performance tests that included in the table are the fabrication of the separator, the performance tests carried out, and the results of the performance tests.

**Table 3. Performance test results from several sources**

Ref.	Fabrication Technique	Performance Test Results		
		Geometry	Mechanical	Electrical
[20]	Modification by adding a layer of phenolic resin (AF) to a commercial separator.	Area shrinkage of 1% to 4%, depending on AF coverage when stored at 135°C for 30 minutes. The separator thickness ranges from 24.50 to 25.54 $\mu\text{m}$ . KSE score 220.7% to 225%. Pore percentage value 47.23% to 58.08%.	Tensile strength is 105.85 MPa with an extension rate of 40.60%-puncture strength up to 4.97 N.	The battery self-discharge retention rate values were 95.67%, 90.41%, 79.48%, and 71.63% after being stored for 8, 24, 40, and 56 days, respectively. The battery discharge capacity holding value is 86%, and the Columbic efficiency is 96.7% after 450 cycles of charging and discharging the battery capacity.
[21]	PLA separator was made by electrospinning technique and then coated with PDA and ZIF.	The thickness of the separator is 40 $\mu\text{m}$ . The contact angle value is 12.9°, with the EAC value up to 290%. The separator does not shrink until it is heated to 165°C.	Young's modulus value of 0.4 GPa.	The ionic conductivity value is $1.99 \times 10^{-3}$ S/cm. The battery discharge capacity holding rate with the studied separator was 98.78% after 200 charge-discharge cycles. This hold rate reduces to 89.03% after 500 cycles. Discharging capacity reaches 140 mAh/g.
[22]	The conventional, wet process mixes PLLA with DMC/DMF to create a pore count.	Pore percentage values range from 71.7% to 74.7%. The most negligible contact angle measurement results are around 61°, with the highest EAC value of 350%.	Young's modulus value is 7.5 MPa.	Ionic conductivity ranges from 0.9 to 1.5 mS/cm. They are discharging capacities rated at 1 C, ranging from 23 to 93 mAh/g, with discharge capacity holding rates between 44% and

Ref.	Fabrication Technique	Performance Test Results		
		Geometry	Mechanical	Electrical
[55]	3D printing using the DIW technique with inks from a mixture of PVDF, N-methyl-2-pyrrolidone, glycerol, and Al <sub>2</sub> O <sub>3</sub> .	Pore percentage values range from 21% to 53%, depending on composition and solvent. Area shrinkage is only 3% to 5% at 190 to 200°C.	The tensile strength ranges from 3.5 to 32.9 MPa, with an increase in pre-fail length of 1.3 to 28.2%.	55%. The ionic conductivity value is 0.0017 to 0.82 mS/cm.
[62]	The conventional, wet process mixes polyvinyl difluoride (PVDF) with polydimethyl siloxane (PDMS), and glycerol and NN dimethyl acetamide (DMAC) as solvents.	The pore size is 1.71 to 13.58 μm with a pore percentage value of 69.33% to 81.53%.	No result	Electrical conductivity values range from 3.45 x 10 <sup>-4</sup> S/cm to 3.20 x 10 <sup>-3</sup> S/cm. Resistance values range from 0.293 to 1.08 Ω.
[64]	The conventional, wet process by mixing Cladophora algae cellulose with H <sub>2</sub> SO <sub>4</sub> solution.	The average thickness is 80 to 176.67 μm. The average pore size is 0.485 to 0.163 μm. No shrinkage occurs when placed at 120°C. The contact angle with liquid electrolyte produces a value of 8.39° to 19.59°.	No result	No result

## 5. CONCLUSION

The use of battery is keep increasing as the use of electrical vehicle increases. As one of the main components, battery has several components that should be developed, one of them is its separator. There are several research conducted that focus on battery separator, start from the development of new material, to the development of new fabrication process for the separator. According to the literature review, there are several materials that are already used as the main material for the separator. One of which that gain attention lately is PLA due to its mechanical strength and temperature stability. Besides, the research trend for this topic, especially for PLA-based separator, is about addition of layer to the existing product or development of new fabrication process of the separator, such as 3D printing. Besides materials, this article also explains the performance testing methods for separator materials, which include the testing apparatus, the measured variables, and the procedures for the experiments.

## REFERENCES

- [1] IEA, "Global Electric Vehicle Outlook 2022," IEA, 2022.
- [2] P. NurHalimah et al., "Battery Cells for Electric Vehicles," *Int. J. Sustain. transp. Technol.*, vol. 2, no. 2, pp. 54–57, Oct. 2019, doi: 10.31427/IJSTT.2019.2.2.3.
- [3] RA Subekti, *Opportunities and challenges in the development of national electric cars*, First printing. Menteng, Jakarta: LIPI Press, 2014.
- [4] Ministry of Investment/BPKM, "Promising Investment in the Indonesian Electric Car Battery Cell Industry Sector," 2022. [Online]. Available: <https://www.bkpm.go.id/id/publikasi/detail/berita/investasi-menjankan-di-sector-industri-sel-baterai-mobil-listrik-indonesia>. [Accessed: Jul. 21, 2022].
- [5] RD Widyantara et al., "Low-Cost Air-Cooling System Optimization on Battery Pack of Electric Vehicles," *Energies*, vol. 14, no. 23, p. 7954, Nov. 2021, doi: 10.3390/en14237954.
- [6] X. Sun, Z. Li, X. Wang, and C. Li, "Technology Development of Electric Vehicles: A Review," *energies*, vol. 13, no. 1, p. 90, Dec. 2019, doi: 10.3390/en13010090.
- [7] M. Aziz, Y. Marcellino, IA Rizki, SA Ikhwanuddin, and JW Simatupang, "STUDY AANALYSIS OF TECHNOLOGY DEVELOPMENT AND SUPPORT OF THE INDONESIAN GOVERNMENT RELATED TO ELECTRIC CARS," *TESLA J. Tek. Electro*, vol. 22, no. 1, p. 45, Mar. 2020, doi: 10.24912/tesla.v22i1.7898.
- [8] MA Hannan, MM Hoque, A. Mohamed, and A. Ayob, "Review of energy storage systems for electric vehicle applications: Issues and challenges," *Renew. sustain. Energy Rev.*, vol. 69, pp. 771–789, Mar. 2017, doi: 10.1016/j.rser.2016.11.171.
- [9] Y. Ding, ZP Cano, A. Yu, J. Lu, and Z. Chen, "Automotive Li-Ion Batteries: Current Status and Future Perspectives," *Electrochem. Energy Rev.*, vol. 2, no. 1, pp. 1–28, Mar. 2019, doi: 10.1007/s41918-018-0022-z.
- [10] D. Bresseret et al., "Perspectives of automotive battery R&D in China, Germany, Japan, and the USA," *J. Power Sources*, vol. 382, pp. 176–178, Apr. 2018, doi: 10.1016/j.jpowsour.2018.02.039.
- [11] Mark T. Demeuse, *Polymer-based Separators for Lithium-ion Batteries: Production, Processing, and Properties*. Amsterdam: Elsevier, 2021.
- [12] LN Putri, RR Alhakim, ARA Ichwan, and E. Retno, "Review: Lithium Ion Battery Separator With Addition of Filler in PVDF/Cellulose Membrane," p. 8.
- [13] J. Choi and PJ Kim, "A roadmap of battery separator development: Past and future," *Curr. Opin. Electrochem.*, vol. 31, p. 100858, Feb. 2022, doi: 10.1016/j.coelec.2021.100858.
- [14] P. Arora and Z. (John) Zhang, "Battery Separators," *Chem. Rev.*, vol. 104, no. 10, p. 4419–4462, Oct. 2004, doi: 10.1021/cr020738u.

- [15] A. Liet *et al.*, “A Review on Lithium-Ion Battery Separators towards Enhanced Safety Performances and Modeling Approaches,” *Molecules*, vol. 26, no. 2, p. 478, Jan. 2021, doi: 10.3390/molecules26020478.
- [16] H. Lee, M. Yanilmaz, O. Toprakci, K. Fu, and X. Zhang, “A review of recent developments in membrane separators for rechargeable lithium-ion batteries,” *Energy Env. sci*, vol. 7, no. 12, p. 3857–3886, 2014, doi: 10.1039/C4EE01432D.
- [17] S. Thiangtham, N. Saito, and H. Manuspiya, “Asymmetric Porous and Highly Hydrophilic Sulfonated Cellulose/Biomembrane Functioning as a Separator in a Lithium-Ion Battery,” *ACS Appl. Energy Mater.*, vol. 5, no. 5, pp. 6206–6218, May 2022, doi: 10.1021/acsaem.2c00602.
- [18] C. Cao, L. Tan, W. Liu, J. Ma, and L. Li, “Polydopamine coated electrospun poly(vinylidene fluoride) nanofibrous membrane as separator for lithium-ion batteries,” *J. Power Sources*, vol. 248, pp. 224–229, Feb. 2014, doi: 10.1016/j.jpowsour.2013.09.027.
- [19] SS Zhang, “A review on the separators of liquid electrolyte Li-ion batteries,” *J. Power Sources*, vol. 164, no. 1, pp. 351–364, Jan. 2007, doi: 10.1016/j.jpowsour.2006.10.065.
- [20] Q. -Q. Gu, H. -J. Xue, Z. -W. Li, J. -C. Song, and Z. -Y. Sun, “High-performance polyethylene separators for lithium-ion batteries modified by phenolic resin,” *J. Power Sources*, vol. 483, p. 229155, Jan. 2021, doi: 10.1016/j.jpowsour.2020.229155.
- [21] L. Deng, C. Cai, Y. Huang, and Y. Fu, “In-situ coating MOFs on 3D-channeled separator with superior electrolyte uptake capacity for ultrahigh cycle stability and dendrite-inhibited lithium-ion batteries,” *Microporous Mesoporous Mater.*, vol. 329, p. 111544, Jan. 2022, doi: 10.1016/j.micromeso.2021.111544.
- [22] J. C. Barbosa *et al.*, “Lithium-ion battery separator membranes based on poly(L-lactic acid) biopolymer,” *Mater. Today Energy*, vol. 18, p. 100494, Dec. 2020, doi: 10.1016/j.mtener.2020.100494.
- [23] J. Cannarella, X. Liu, CZ Leng, PD Sinko, GY Gor, and CB Arnold, “Mechanical Properties of a Battery Separator under Compression and Tension,” *J. Electrochem. Soc.*, vol. 161, no. 11, p. F3117–F3122, 2014, doi: 10.1149/2.0191411jes.
- [24] MK Aslamet *et al.*, “How to avoid dendrite formation in metal batteries: Innovative strategies for dendrite suppression,” *Nano Energy*, vol. 86, p. 106142, Aug. 2021, doi: 10.1016/j.nanoen.2021.106142.
- [25] L. Frenck, GK Sethi, JA Maslyn, and NP Balsara, “Factors That Control the Formation of Dendrites and Other Morphologies on Lithium Metal Anodes,” *Front. Energy Res.*, vol. 7, p. 115, Nov. 2019, doi: 10.3389/fenrg.2019.00115.
- [26] LA Selis and JM Seminario, “Dendrite formation in silicon anodes of lithium-ion batteries,” *RSC Adv.*, vol. 8, no. 10, p. 5255–5267, 2018, doi: 10.1039/C7RA12690E.



- [27] MC Ma, G. Li, X. Chen, LA Archer, and J. Wan, "Suppression of dendrite growth by cross-flow in microfluidics," *Sci. Adv.*, vol. 7, no. 8, p. eabf6941, Feb. 2021, doi: 10.1126/sciadv.abf6941.
- [28] C. Martinez-Cisneros, C. Antonelli, B. Levenfeld, A. Varez, and J. -Y. Sanchez, "Evaluation of polyolefin-based macroporous separators for high temperature Li-ion batteries," *Electrochimica Acta*, vol. 216, pp. 68–78, Oct. 2016, doi: 10.1016/j. electacta.2016.08.105.
- [29] B. Junget *et al.*, "Thermally stable non-aqueous ceramic-coated separators with enhanced nail penetration performance," *J. Power Sources*, vol. 427, pp. 271–282, Jul. 2019, doi: 10.1016/j.jpowsour.2019.04.046.
- [30] KJ Kim, M. Balaish, M. Wadaguchi, L. Kong, and JLM Rupp, "Solid-State Li–Metal Batteries: Challenges and Horizons of Oxide and Sulfide Solid Electrolytes and Their Interfaces," *Adv. Energy Mater.*, vol. 11, no. 1, p. 2002689, Jan. 2021, doi: 10.1002/aenm.202002689.
- [31] A. Saal, T. Hagemann, and US Schubert, "Polymers for Battery Applications—Active Materials, Membranes, and Binders," *Adv. Energy Mater.*, vol. 11, no. 43, p. 2001984, Nov. 2021, doi: 10.1002/aenm.202001984.
- [32] M. Yang and J. Hou, "Membranes in Lithium Ion Batteries," *membranes*, vol. 2, no. 3, pp. 367–383, Jul. 2012, doi: 10.3390/membranes2030367.
- [33] Celgard, "Celgard's Products Data." [On line]. Available: <https://www.celgard.com/product-data>. [Accessed: Aug. 01, 2022].
- [34] Entek Membrane LLC, "Entek's Products." [On line]. Available: <https://entek.com/lithium/products/>. [Accessed: Aug. 01, 2022].
- [35] Entek Membrane LLC, *Separator Product Portfolio*. Entek Membrane LLC.
- [36] Asahi-Kasei, "Asahi-Kasei's Products." [On line]. Available: [https://www.asahi-kasei.com/services\\_products/search/#material?category1=4](https://www.asahi-kasei.com/services_products/search/#material?category1=4). [Accessed: Aug. 01, 2022].
- [37] X. Zuo *et al.*, "Bubble-template-assisted synthesis of hollow fullerene-like MoS<sub>2</sub> nanocages as a lithium ion battery anode material," *J. Mater. Chem. A*, vol. 4, no. 1, pp. 51–58, 2016, doi: 10.1039/C5TA06869J.
- [38] Y. Liu *et al.*, "3D printed separator for the thermal management of high-performance Li metal anodes," *Energy Storage Mater.*, vol. 12, p. 197–203, May 2018, doi: 10.1016/j.ensm.2017.12.019.
- [39] C. Liao *et al.*, "A flame-retardant, high ionic-conductivity and eco-friendly separator prepared by papermaking method for high-performance and superior safety lithium-ion batteries," *Energy Storage Mater.*, vol. 48, pp. 123–132, Jun. 2022, doi: 10.1016/j.ensm.2022.03.008.

- [40] J. Qian *et al.*, “Toward stretchable batteries: 3D-printed deformable electrodes and separator enabled by nanocellulose,” *Mater. Today*, vol. 54, pp. 18–26, Apr. 2022, doi: 10.1016/j.mattod.2022.02.015.
- [41] SC Mun and JH Won, “Manufacturing Processes of Microporous Polyolefin Separators for Lithium-Ion Batteries and Correlations between Mechanical and Physical Properties,” *Crystals*, vol. 11, no. 9, p. 1013, Aug. 2021, doi: 10.3390/cryst11091013.
- [42] CJ Weber, S. Geiger, S. Falusi, and M. Roth, “Material review of Li ion battery separators,” presented at the REVIEW ONELECTROCHEMICAL STORAGE MATERIALS AND TECHNOLOGY: Proceedings of the 1st International Freiberg Conference on Electrochemical Storage Materials, Freiberg, Germany, 2014, pp. 66–81, doi: 10.1063/1.4878480 [Online]. Available: <http://aip.scitation.org/doi/abs/10.1063/1.4878480>. [Accessed: Sept. 07, 2022].
- [43] T. Wu, K. Wang, M. Xiang, and Q. Fu, “Progresses in Manufacturing Techniques of Lithium-Ion Battery Separators in China,” *Chin. J. Chem.*, vol. 37, no. 12, p. 1207–1215, Dec. 2019, doi: 10.1002/cjoc.201900280.
- [44] T. Wu, M. Xiang, Y. Cao, J. Kang, and F. Yang, “Pore formation mechanism of  $\beta$  nucleated polypropylene stretched membranes,” *RSC Adv*, vol. 4, no. 69, pp. 36689–36701, 2014, doi: 10.1039/C4RA03589E.
- [45] L. Ding, R. Xu, L. Pu, F. Yang, T. Wu, and M. Xiang, “Pore formation and evolution mechanism during biaxial stretching of  $\beta$ -iPP used for lithium-ion battery separator,” *Mater. Dec.*, vol. 179, p. 107880, Oct. 2019, doi: 10.1016/j.matdes.2019.107880.
- [46] G. Shi, F. Chu, G. Zhou, and Z. Han, “Plastic deformation and solid-phase transformation in  $\beta$ -phase polypropylene,” *Makromol. Chem.*, vol. 190, no. 4, pp. 907–913, Apr. 1989, doi: 10.1002/macp.1989.021900423.
- [47] Xiangyun Wei and Charles Haire, “Biaxially Oriented Microporous Membrane,” US008795565B2.
- [48] Z. Lyue *et al.*, “Design and Manufacture of 3D-Printed Batteries,” *Joule*, vol. 5, no. 1, pp. 89–114, Jan. 2021, doi: 10.1016/j.joule.2020.11.010.
- [49] A. Maurelet *et al.*, “Three-Dimensional Printing of a LiFePO<sub>4</sub>/Graphite Battery Cell via Fused Deposition Modeling,” *Sci. Rep.*, vol. 9, no. 1, p. 18031, Dec. 2019, doi: 10.1038/s41598-019-54518-y.
- [50] C. Reyes *et al.*, “Three-Dimensional Printing of a Complete Lithium Ion Battery with Fused Filament Fabrication,” *ACS Appl. Energy Mater.*, p. acaem.8b00885, Oct. 2018, doi: 10.1021/acsaem.8b00885.
- [51] C. Yuan, L. Wang, S. Yin, and J. Xu, “Generalized separator failure criteria for internal short circuit of lithium-ion battery,” *J. Power Sources*, vol. 467, p. 228360, Aug. 2020, doi: 10.1016/j.jpowsour.2020.228360.

- [52] National Institute of Standards and Technology, "Scanning Electron Microscope with Spin Polarization Analysis," *Wikimedia Commons*. [On line]. Available: [https://commons.wikimedia.org/wiki/File:Scanning\\_Electron\\_Microscope\\_with\\_Spin\\_Polarization\\_Analysis\\_\(5941086294\).jpg](https://commons.wikimedia.org/wiki/File:Scanning_Electron_Microscope_with_Spin_Polarization_Analysis_(5941086294).jpg).
- [53] Kerina yin, "Tensile testing on a coir composite," *Wikimedia Commons*. [On line]. Available: [https://commons.wikimedia.org/wiki/File:Tensile\\_testing\\_on\\_a\\_coir\\_composite.jpg](https://commons.wikimedia.org/wiki/File:Tensile_testing_on_a_coir_composite.jpg).
- [54] DV Ribeiro *et al.*, "Effect of Red Mud on the Corrosion of Reinforced Concrete Studied by Electrochemical Impedance Spectroscopy," *ISRN Mater. Sc.*, vol. 2011, pp. 1–11, Oct. 2011, doi: 10.5402/2011/365276.
- [55] AJ Blake *et al.*, "3D Printable Ceramic–Polymer Electrolytes for Flexible High-Performance Li-Ion Batteries with Enhanced Thermal Stability," *Adv Energy Mater*, p. 10, 2017.
- [56] A. Mahendra and ZAI Supardi, "A REVIEW: ELECTROCHEMICAL IMPEDANCE SPECTROSCOPIES AND ITS APPLICATIONS IN LITHIUM-ION BATTERIES," *inov. Fis. Indonesia.*, vol. 10, no. 2, pp. 59–67, Jul. 2021, doi: 10.26740/ifi.v10n2.p59-67.
- [57] S. Wang, J. Zhang, O. Gharbi, V. Vivier, M. Gao, and ME Orazem, "Electrochemical impedance spectroscopy," *Nat. Rev. Primary Methods*, vol. 1, no. 1, p. 41, Dec. 2021, doi: 10.1038/s43586-021-00039-w.
- [58] ST Manik and E. Taer, "Impedance Spectroscopy of Supercapacitor Cells using Monolithic Carbon Electrodes from Sugarcane Bagasse," p. 7.
- [59] Kruss Scientific, "Drop Shape Analyzer-DSA100E," *Drop Shape Analyzer-DSA100E*. [On line]. Available: <https://www.kruss-scientific.com/en/products-services/products/dsa100e>. [Accessed: Sept. 15, 2022].
- [60] ATA Scientific Instruments, "Attention Theta Flex." [On line]. Available: <https://www.atascientific.com.au/products/attention-theta/>. [Accessed: Sept. 15, 2022].
- [61] Biolin Scientific, "Standards for Tensiometers." [On line]. Available: <https://www.biolinscientific.com/attention/standards-for-tensiometers#optical-tensiometers>. [Accessed: Sept. 13, 2022].
- [62] DES Arifin, M. Zainuri, and JARHakim, "Characterization of the Properties of PVDF/poly(dimethylsiloxane) Composite Separator Using the Blending Membrane Method," vol. 3, p. 5, 2014.
- [63] EM Wigayati, I. Purawardi, and Q. Sabrina, "Surface Morphological Characteristics of Polymer PVdF-LiBOB-ZrO<sub>2</sub> and Its Potential for Lithium Battery Electrolytes," *J. Kim. And Packaging*, vol. 40, no. 1, p. 1, Feb. 2018, doi: 10.24817/jkk.v0i0.3028.
- [64] AN Fauza, MM Mardiyati, and S. Steven, "MAKING AND CHARACTERIZATION OF CELLULO BATTERY SEPARATORSSA ALGA CLADOPHORA," *J. Teknol. Materials And Goods Tech.*, vol. 9, no. 2, p. 69, Dec. 2019, doi: 10.37209/jtbbt.v9i2.135.

- [65] National Institute of Standards and Technology, "FTIR Spectroscopy." [On line]. Available: <https://webbook.nist.gov/chemistry/special/spray-combust/baseline-case/ftir/>. [Accessed: Dec. 20, 2022].
- [66] P.Baiet *al.*, "Interactions between Lithium Growths and Nanoporous Ceramic Separators," *Joule*, vol. 2, no. 11, p. 2434–2449, Nov. 2018, doi: 10.1016/j.joule.2018.08.018.
- [67] D. Aurbach, "A short review of failure mechanisms of lithium metal and lithiated graphite anodes in liquid electrolyte solutions," *Solid State Ion.*, vol. 148, no. 3–4, pp. 405–416, Jun. 2002, doi: 10.1016/S0167-2738(02)00080-2.